Global NEST Journal, Vol 25, No 10, pp 124-131

Entrapment of green seaweed *Caulerpa scalpelliformis* for extracting Pb(II), Ni(II) and Zn(II) metal ions from aqueous solutions

Zunaithur Rahman D.[1], Thiru S.[2], Kousalyadevi G.[3]* and Hariharan T.[4]

[1]Department of Civil Engineering, Aalim Muhammed Salegh College of Engineering, Chennai - 600055, Tamil Nadu, India.

[2]Department of Mechanical and Materials Engineering, University of Jeddah, Jeddah - 21959, Kingdom of Saudi Arabia.

[3]School of Architecture and Interior Design, SRM Institute of Science and Technology, kattankulathur campus - 603203, Tamilnadu, India.

[4]Department of Chemical Engineering, Mohamed Sathak Engineering College, Kilakarai 623806, Tamil Nadu, India

Received: 28/08/2023, Accepted: 09/10/2023, Available online: 23/10/2023

*to whom all correspondence should be addressed: e-mail: kousym.arch@gmail.com

https://doi.org/10.30955/gnj.005335

Graphical abstract

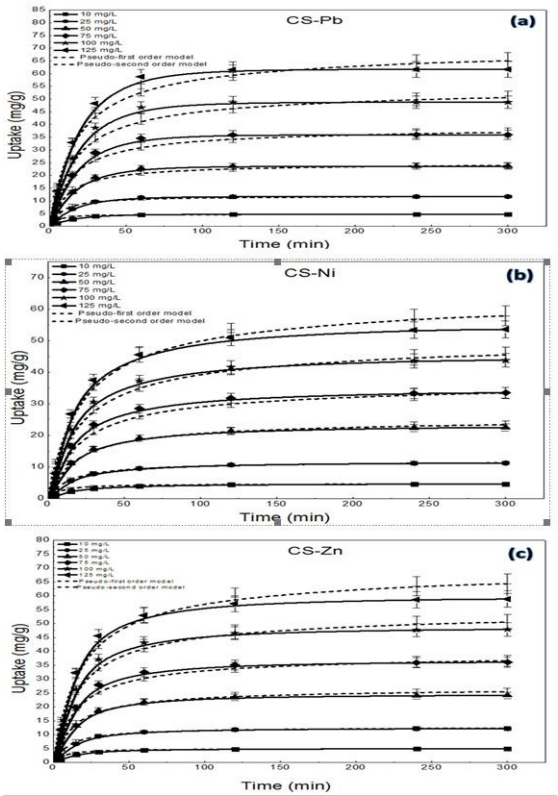

Abstract

From this study, green seaweed *Caulerpa Scalpelliformis* is utilized as a sorbent for the removal of three metals such as lead (Pb), nickel (Ni) and zinc (Zn). Adsorption tests showed that maximum removal efficiency of 75.02% for Pb, 80% for Ni and 91.11% for Zn was obtained at an optimal equilibrium pH of 7 for Pb and 6 for Ni, Zn, 2g/L sorbent at an ionic strength of 100 mg/L of 30°C. Four isotherm models, such as Langmuir, Freundlich, Toth, and Sips used in this study to determine the correct fit model from test results. The toth model (R^2=0.999) was well fit compared to other isotherms models based on correlation coefficients. Kinetic model results obtained at initial Pb, Ni and Zn concentrations revealed a high biosorption rate. In contrast, the results have been modelled effectively with the pseudo-first and second orders. As a result, tests with elutants found that 0.1M HCl is the perfect desorption elutant for three metal ions.

Keywords: Biosorption, green seaweed, metal, sustainability, wastewater.

1. Introduction

Heavy metal ions are considered carcinogenic and poisonous (Xu and Duran 2018). Metal ions close to water, air, soil, and structural integrity and highly resist microbial environmental degradation (Vijayaraghavan *et al.* 2017; Kanagaraj *et al.* 2015). By inhibiting the water supply's re-oxygenating ability by sunlight, largely concentrated metal ions in bodies deteriorated the bioactive function of water bodies and the photosynthesis cycle of plants or algae (Maiti *et al.* 2019; Li *et al.* 2017). Metal ions present significant threats to human well-being, including the breakdown of the reproductive system and cause severe damage to the brain, central nervous system, liver and kidney (Yusuf 2018; Vijayaraghavan and Ashokkumar 2017).

Some heavy metals will kill the DNA, which can cause malignant tumours. Recent works have shown that heavy metals can contribute to breathing and skin allergy (Mazur *et al*. 2018; Liu *et al.* 2019). The literature has also documented evidence for developing liver, urinary and kidney cancer in work after continuous exposure to metal ions affect tissues (Ravindiran *et al.* 2019). It is, therefore, necessary to eliminate these toxic metal ions from wastewater before disposal.

Numerous practical techniques have been used in wastewater treatment for metal ion isolation. These

approaches include the Exchange of ions, radiation, adsorption, electrokinetic coagulation, and filtration from membranes. Oxidation, ozone, and photochemical methods are required for chemical processes used to remediate metal pollution (Gokulan *et al.,* 2019). Biological methods used in metal-containing wastewater have been the focus of recent work (Gokulan *et al.* 2019). Biomaterials have been used in biological systems to detoxify organic/inorganic toxins. Metal recovery utilizing biosorption has been extensively reported in recent years (Prodromou and Pashalidis 2015; Gao *et al.* 2018). Bioaccumulation-another metal remediation, also a cellular method, involves the removal of toxins by the healthy cells. Bioaccumulation consists of two-stage of quick sorbate sorption in the cell portion of the biomass and then slower active absorption of the sorbate based on the metabolism (Gupta *et al.* 2018; Cecen 2018).

The adsorption of dye from aqueous solution using *Caulerpa Scalpelliformis* (CS) is examined by Aravindhan, Rao and Nair 2007; Gokulan, Prabhu and Jegan 2019. For limited research work, *C.Scalpelliformis* was used as an adsorbent for wastewater removal pollutants. Therefore, the main objective of this study is to generate a sorbent *C.Scalpelliformis* from green Seaweed and to explore their ability to be used in the remediation of metal ions from aqueous solutions. To the best of our understanding, this is the first research being proposed for the production and remediation of lead (Pb), nickel (Ni) and zinc (Zn) ions by *Caulerpa Scalpelliformis*.

2. Materials and methods

2.1. Seaweeds collection and chemicals

Caulerpa Scalpelliformis, used in the research, was obtained from the southern coast of Tamilnadu, India. The collected Seaweed was rinsed with deionized water and ten days of sunlight contacts and incurred for 6 hours at 105°C in the oven, cut into small pieces and pulverized using a domestic mixer (1HP Micro active, India). Dry biomass was grounded and sieved to produce 150 to 175 µm of *C.Scalpelliformis* particles. Heavy metals such as Pb, Ni, and Zn have been included in the research and are purchased from MERCK (India).

2.2. Sorbent characterization

The sorbent surface properties have been examined using Scanning Electron Microscopy (SEM) (JEOL JSM 6360 Japan). On samples before SEM analysis, a thin film of platinum was covered. A Fourier Transform Infrared (FT-IR) spectrophotometer (Perkin Elmer, Spectrum RX1) was used to evaluate the surface functionality of different sorbent samples. Before FT–IR examination, dry sorbent samples were combined with KBr forms pellets. The multipoint Brunauer determined the pore diameter/radius and surface area–Emmett–Teller analyzer (Autosorb IQ Station 1).

2.3. Metal Ions adsorption studies

Batch experiments were planned to refine the basic process parameters for optimum sorption efficiency. In the case of a sorbent dose, the required ion concentration (100 mL) was normally transferred to a 250 mL Erlenmeyer flake. The material was well balanced and mixed with 150 rpm in a rotary shaker (PS Instruments, India). The flask suspension was centrifuged for 3 minutes at 4000 rpm after the equilibrium between the sorbent and metal ions had ended in 4 hours. The concentration of metal ions from the supernatant was calculated using atomic absorption spectroscopy (AAS Vario 6, Analytik Jena, Germany). The tests were repeated by varying different parameters.

2.4. Modeling of isotherm and kinetics data

The absorption of metal ions by sorbent was determined by the formula (1)

$$Q = V(C_0 - C_e)/W \quad (1)$$

Where V is the volume of the metal solution (L), Q is the sorbent capacity (mg/L), C_0 is the initial metal concentration (mg/L), C_e is the equilibrium concentration (mg/L), and W is the weight of *C.Scalpelliformis* (g).

The efficiency of the metal removal (%) was estimated by the formula (2),

$$Removal\ efficiency = \frac{(C_0 - C_e)}{C_0} \times 100 \quad (2)$$

To fit the isotherm data, four different isotherm models have been used, expressed in equations (3-6),

$$\text{Freundlich model:} \quad Q = K_F C_e^{1/n_F} \quad (3)$$

$$\text{Langmuir model:} \quad Q = \frac{Q_{max} b_L C_e}{1 + b_L C_e} \quad (4)$$

$$\text{Toth model:} \quad Q = \frac{Q_{max} b_T C_e}{[1 + (b_T C_e)^{1/n_T}]^{n_T}} \quad (5)$$

$$\text{Sips model:} \quad Q_e = \frac{K_S C_e^{\beta_S}}{1 + a_S C_e^{\beta_S}} \quad (6)$$

In case n_F is an exponent of the Freundlich model, K_F is the Freundlich model coefficient (L/g)$1/n_F$, Q_{max} is the maximum metal ion uptake by *C.Scalpelliformis* (mg/L), b_L is the Langmuir model equilibrium coefficient (L/mg), b_T is the Toth model constant (L/mg), n_T represents a Toth model exponent, a_S is the Sips model coefficient, β_S is the exponent of Sips model (L/mg).

Two kinetic models expressed in equations (7) and (8) were used to describe sorption kinetics.

$$\text{Pseudo-first order model:} \quad Q_t = Q_e(1 - \exp(-k_1 t)) \quad (7)$$

$$\text{Pseudo-second order model:} \quad Q_t = \frac{Q_e^2 k_2 t}{1 + Q_e k_2 t} \quad (8)$$

When Q_e is the equilibrium metal uptake capacity (mg/g), Q_t is the metal uptake capacity of the pseudo-first and pseudo-second-order models at every time t (mg/g) such as k_1 (1/min) and k_2 (g/mg.min) respectively.

The parameters of the different models were calculated using the Sigma-plot (V4.0, SPSS, USA) software with a nonlinear regression technique (Chen *et al.* 2018).

2.5. Elution and regeneration

Desorption of C.Scalpelliformis was tested by some elutants, including 0.1 M HCl, H_2SO_4 and HNO_3, and 0.1 $CaCl_2$.

3. Results and discussion

3.1. Characterization of C. Scalpelliformis

Figure 1 displays the SEM photos of virgin *C.Scalpelliformis* and separate Pb, Ni, and Zn-bound sorbent samples. The raw sorbent surface is usually considered to be smooth. Important differences were noticed on the surface of the sorbent after it was filled with various metal ions. This means an ion exchange has arisen between the sorbent and the metal ions (Rahman *et al.* 2017).

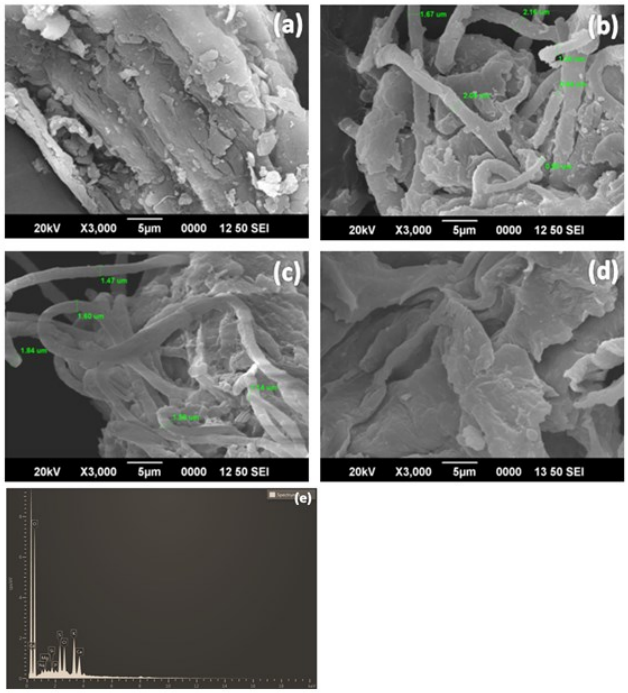

Figure 1. *Scanning electron micrographs of C.Scalpelliformis (a), C.Scalpelliformis loaded Pb (b), Ni (c), Zn (d) and SEM-EDS of C.Scalpelliformis (e)*

FT-IR spectra of *C.Scalpelliformis* and metal-loaded sorbent samples were contrasted by considering the essence of the matrix bond involved with removing metal ions. The sorbent FT-IR continuum verified the presence of broad bands at 1025.94 (C-O (alcohol) band), 1414.53 (symmetric C=O), 1607.38 (asymmetric C=O COOH stretch), 2928.38 (C-H stretch) and 3333.36 (-NH,-OH stretch) in Figure 2. It was proved that the sorbent consisted of binding sites of diverse nature with the above-mentioned spectral peaks. The FT-IR spectra of metal-bound sorbent demonstrated large differences in sorbent functional properties due to the ions' interaction between sorbent and metal ions. The FTIR spectrum also indicated the potential presence of electrostatic interacting metal ions of many functional groups on the sorbent surface (Rangabhashiyam *et al.* 2016). Table 1 lists the significant changes in the sorbent samples of all three metal ions studied.

Energy-dispersive X-ray spectroscopy (EDS) evaluation showed this raw *C.Scalpelliformis* composed of large amounts of oxygen (84.94%), potassium (4.50%) and sulfur (2.93%) (Deng *et al.* 2016). BET study shows the improved surface area (3.792 m^2/g), pore volume ($4.350x10^{-3}cm^3/g$) and pore size (2.29 nm) of *C.Scalpelliformis* and influence in adsorption capability (Torab *et al.* 2013).

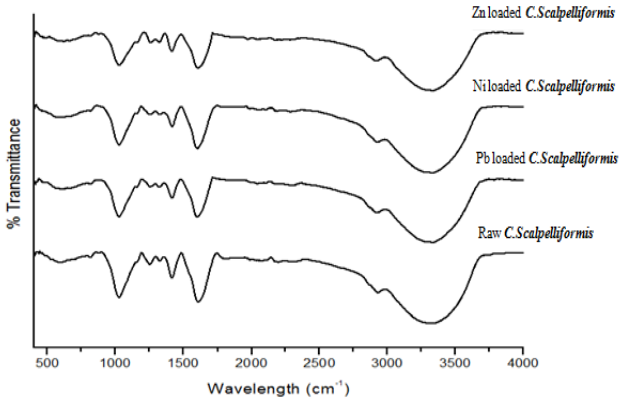

Figure 2. *FT-IR spectra of raw and metal loaded C.Scalpelliformis*

Table 1. *FT-IR spectra stretching frequencies as detected in raw and metal loaded C.Scalpelliformis*

Assignment	Wavenumber (cm^{-1})			
	Raw Seaweed	Pb loaded Seaweed	Ni loaded Seaweed	Zn loaded Seaweed
–OH, –NH stretching	3333.36	3337.21	3332.39	3334.32
Asymmetric CH_2 stretching	2928.38	2923.56	2926.45	2922.59
–P–H– group	2319.95	2281.38	2287.16	2191.70
Asymmetric C=O stretch of COOH	1607.38	1600.63	1600.63	1604.48
Symmetric C=O	1414.53	1414.53	1416.46	1413.57
C–O (COOH) stretching	1251.58	1254.47	1252.54	1256.40
C=C stretching	1145.38	1145.19	1147.16	1144.48
C–O (alcohol) band	1025.94	1024.98	1025.94	1026.91
C=O of aromatic stretching	871.67	874.56	-	870.74
Alkane group	596.86	614.22	616.15	620.00

3.2. Equilibrium pH influence on the adsorption

pH performs a very significant function in absorbing all three metal ions. pH effect was examined by changing the pH conditions from 2 to 9 (Figure 3). The findings showed that the rise in pH improved the loss of percent of metal ions. For instance, the uptake capacity of 2.166 mg/g and the removal efficiency of 10.83% at pH 2 for Pb increased to 75.02% at pH 7.0. For example, with a pH increase from 2.0 to 6.0, the Ni and Zn uptake ability increased by 80.00% and 91.12%, while a pH increase from 6.0 to 9.0 decreased uptake ability by 57.58% 38.39% for Ni and Zn (Figure 3). Metal ions and sorbent surfaces are prone to electrostatic interactions, which results in a rise in the sorption of Pb, Ni and Zn at low pH (Deng *et al.* 2016; Senthilkumar *et al.* 2017). In the adsorption batch tests, pH 7.0 for Pb, 6.0 for Ni and Zn were defined as functional and optimum pH for the adsorption of three metal ions by *C.Scalpelliformis*.

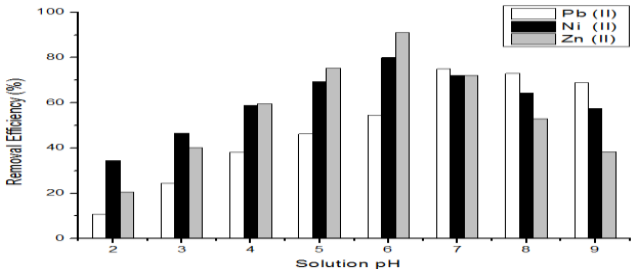

Figure 3. *Equilibrium pH influence on metal adsorption of C.Scalpelliformis for Pb, Ni, and Zn (Conditions: C_o = 100 mg/L; D_o = 5 g/L)*

3.3. Sorbent dosage impact on adsorption

Sorbent dose increases from 2 to 10 g/L analyzed the impact of the sorbent dose on the sorption of three metal ions. In contrast, the pH and initial metal concentrations were held at 7 for Pb and 6 for Ni, Zn, and 100 mg/L, respectively. Figure 4 indicates that the absorption potential of metal ions reduces with a rise in sorbent concentration. It is attributed to the assumption that at a reduced dose, the binding ability of all particles in the sorbent is improved in the absorption potential of the metal ions. Still, at a higher dose agglomeration, the critical function of the sorbent may reduce. For example, when the sorbent dose was raised from 2 g/L to 10 g/L, the absorption ability of the metal ions was improved by *C.Scalpelliformis*-sorbent decreased from 44.325 to 4.387 mg/L (Pb), 43.830 to 4.353 mg/L (Ni), 47.886 to 7.013 mg/L (Zn), respectively.

Conversely, the exclusion performance of *C.Scalpelliformis*-sorbent improved from 43.87 to 88.65% for Pb, 43.53 to 87.66% for Ni, 70.13 to 95.77% for Zn, respectively, after growing the volume of sorbent from 2 to 10 g/L (Figure 4). The increased sorbent surface area could be attributed to the highest adsorption (Rangabhashiyam *et al.* 2014). The optimal dose is then measured as 2g/L and calculated based on the metal removal percentage and adsorbent uptake performance.

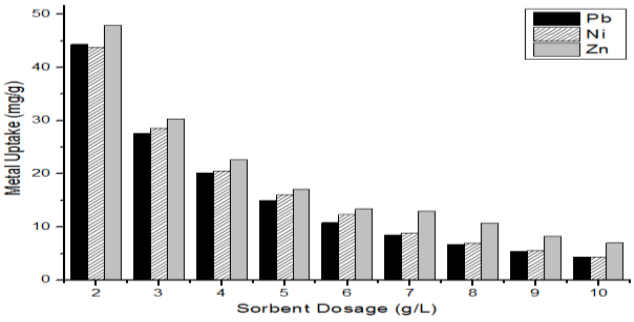

Figure 4. *Sorbent dosage impact on metal adsorption of C.Scalpelliformis for Pb, Ni and Zn (Conditions: pH = 7 for Pb, 6 for Ni and Zn, C_o = 100 mg/L)*

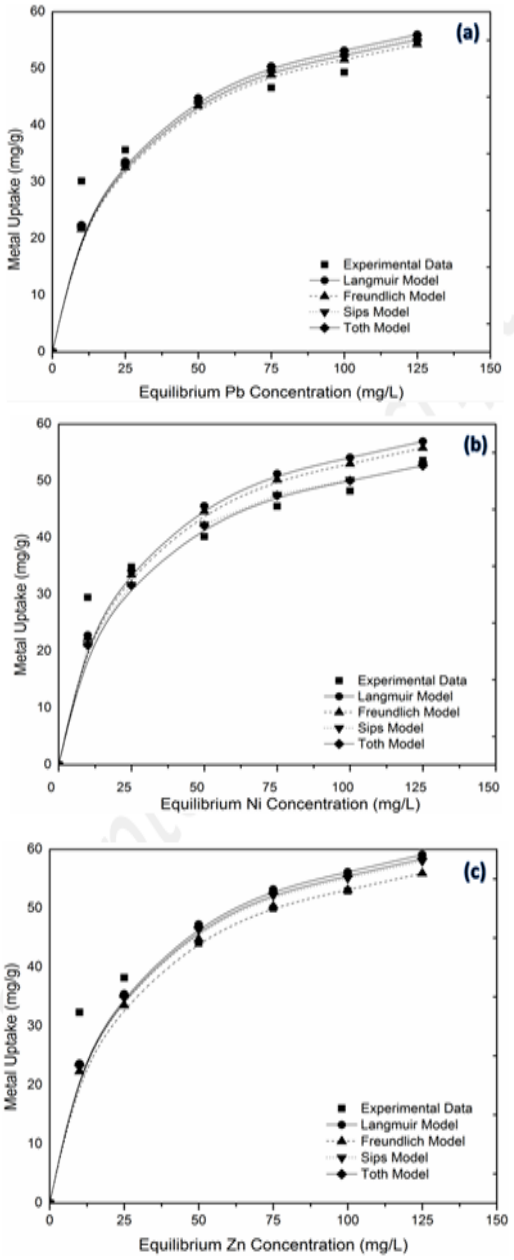

Figure 5. *Metal ion sorbent isotherms interaction with C. Scalpelliformis in Pb, Ni and Zn (Conditions: D_o = 2 g/L, pH = 7.0 for Pb, 6.0 for Ni and Zn)*

3.4. Sorption Isotherms

Sorption isotherm is very important if the whole adsorbent potential and its affinity with sorbates are to be

understood (Sagar and Rastogi 2019; Praveen and Vijayaraghavan 2014). Isotherm sorption was detected at a constant pH of 7 for Pb and 6 for Ni and Zn at 30°C at different initial metal ion concentrations of 10, 25, 50, 75, 100, and 125 mg/L. Figure 5 shows that the increase in the initial concentration increased the potential for *C. scalpelliformis* metal sorption. Initial steep inclination in the isotherm curve for all three metals examined showed the sorbent derived from *C. Scalpelliformis*, indicating a high affinity between the sorbent and three metal ions. The maximum sorbent metal ion uptake capacities for Pb, Ni and Zn were measured at 44.325, 43.830 and 47.886 mg/g using isotherm result data.

Table 2. *Model isotherm parameters in the Pb, Ni and Zn adsorption on C.scalpelliformis*

Models		Unit	Pb	Ni	Zn
Langmuir	Q_{max}	mg/L	40.073	48.848	51.998
	b_L	L/mg	0.121	0.144	0.196
	R^2	-	0.913	0.910	0.913
Freundlich	K_F	$(L/g)1/n_F$	6.069	7.536	8.355
	n_F	L/mg	0.511	0.559	0.575
	R^2	-	0.991	0.989	0.982
Sips	K_S	$(L/g)1/n_F$	20.209	22.320	29.854
	a_S	L/mg	0.284	0.308	0.345
	β_S	L/mg	0.985	1.069	1.039
	R^2	-	0.997	0.995	0.995
Toth	Q_{max}	mg/L	44.494	55.815	57.032
	b_T	L/mg	0.168	0.197	0.275
	n_T	L/mg	2.560	2.893	3.006
	R^2	-	0.999	0.999	0.998

The effects of the metal ion isotherms are described in the Freundlich, Langmuir, Sips and Toth models, and the impact is presented in Figures 6 and 2. The Freundlich analysis showed that the isothermal data had a strong correlation coefficient (>0.982) (Table 2). The K_F and n_F for *C.Scalpelliformis* can be derived from Table 2 in the following order: Zn>Ni>Pb. In comparison, using the Langmuir model, isotherm data across the entire range were clearer to be defined using relatively low coefficients of correlation (> 0.910), as shown in Table 2 of this article. The Q_{max} value of sorbent was reported for Zn (51.998 mg/g), accompanied by Ni (48.848 mg/g) and Pb (40.073 mg/g). Similarly, affinity constant (b_L) values were found in the following order: Zn (0.196 L/mg) > Ni (0.144 L/mg)> Pb (0.121 L/mg).

In the Sips model, experimental with small and high correlation coefficients (>0.997) have been very strongly forecast (Table 2). Constant binding and affinity values were observed for Zn, followed by Ni and Pb. The Toth model culminated in the strongest estimate of the isotherm models tested with the maximum correlation coefficient (>0.999). Compared to other test performances, the maximum constants of the Toth model were obtained for Zn, accompanied by Ni and Pb (Table 3). Compared to experimental isotherm results, Figure 5 shows the expected curves of all four models.

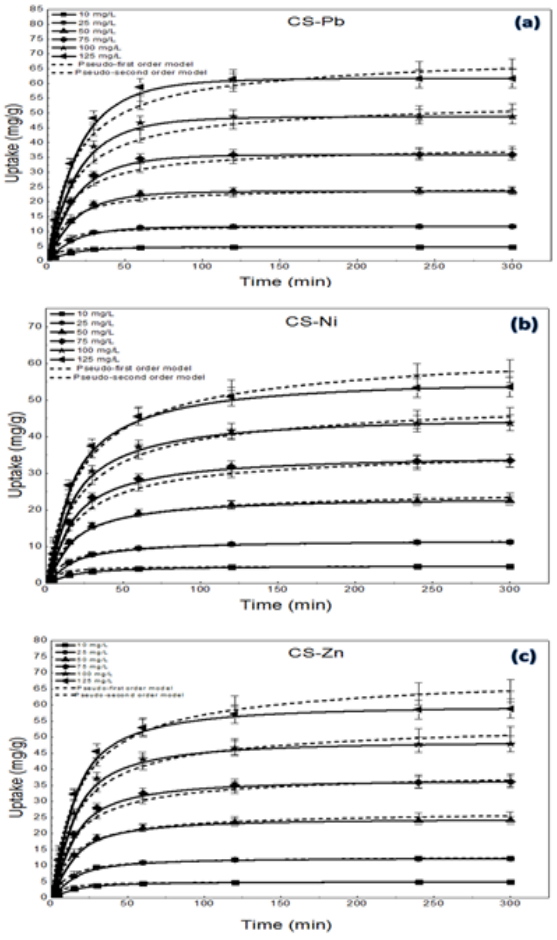

Figure 6. Biosorption Kinetics of Pb (a), Ni (b) and Zn (c) during interaction with C.Scalpelliformis by pseudo models (Conditions: D_o = 2 g/L, pH = 7.0 for Pb, 6.0 for Ni and Zn)

3.5. Sorption kinetics

Kinetic experiments have increased the concentration of initial metal ions from 10-125 mg/L at a pH of 7 for Pb and 6 for Ni and Zn at room temperature. The results show that during the first 120 minutes, the rate of metal sorption was considered moderate, and the adsorption rate decreased over a longer period with the final equilibrium achieved. It was also clear that increased metal ion levels improved the metal-sorbent adsorption equilibrium (Table 3). The sorbent extracted from *C.Scalpelliformis* obtained 99.5% of overall Pb sorption within 120 min of initial Pb concentration of 10 to 125 mg/L. The equilibrium time for all three metals at different initial concentrations was then determined to be 240 minutes (Figure 6). Furthermore, results have shown that the overall sorbent efficiency of the *C.Scalpelliformis* has been greatly impaired by the initial metal ion concentration, as increased adsorption of metal ions (Hua *et al.* 2019) (Table 3). For example, the sorption ability of Zn and Ni by *C.Scalpelliformis* improved from 11.76 to 58.82 mg/L (97.25%) and 8.04 to 53.59 mg/L (95%), while the concentration of Zn and Ni from 10 to 125 mg/L.

Table 3. *PFO and PSO kinetic parameters during Pb, Ni and Zn sorption on C.Scalpelliformis*

Metal	Model	Model constants	Unit	10 mg/L	25 mg/L	50 mg/L	75 mg/L	100 mg/L	125 mg/L
Pb	Pseudo-first-order model constants	Q_e	mg/g	4.7298	11.6788	23.5987	35.9695	48.7575	61.6950
		k_1	1/min	0.0620	0.0578	0.0556	0.0554	0.0562	0.0590
		R^2	-	0.9988	0.9998	0.9988	0.9948	0.9967	0.9966
	Pseudo-second-order model constants	Q_e	mg/g	4.7767	11.9637	24.7225	38.4790	53.1900	68.5500
		k_2	g/mg.min	0.0626	0.0152	0.0004	0.0002	0.0021	0.0090
		R^2	-	0.8670	0.9662	0.9891	0.9895	0.9833	0.9817
Ni	Pseudo-first-order model constants	Q_e	mg/g	4.6793	11.5517	23.6344	36.0231	48.2127	60.2894
		k_1	1/min	0.0465	0.0474	0.0423	0.0481	0.0450	0.0329
		R^2	-	0.9913	0.9943	0.9973	0.9973	0.9953	0.9903
	Pseudo-second-order model constants	Q_e	mg/g	4.7257	11.8335	24.7599	38.5365	52.5960	66.9888
		k_2	g/mg.min	0.0314	0.0046	0.0032	0.0031	0.0090	0.0070
		R^2	-	0.9163	0.9867	0.9903	0.9951	0.9900	0.9879
Zn	Pseudo-first-order model constants	Q_e	mg/g	4.9884	12.4630	25.3375	38.7591	52.6746	66.1690
		k_1	1/min	0.0552	0.0531	0.0459	0.0487	0.0436	0.0484
		R^2	-	0.9927	0.9927	0.9950	0.9990	0.9965	0.9954
	Pseudo-second-order model constants	Q_e	mg/g	5.0378	12.7670	26.5441	41.4633	57.4632	73.5213
		k_2	g/mg.min	0.0384	0.0028	0.0003	0.0071	0.0011	0.0080
		R^2	-	0.9350	0.9870	0.9907	0.9946	0.9849	0.9837

Pseudo-first (PFO) and pseudo-second-order (PSO) models matched and tested *C.Scalpelliformis*-metal ion kinetics. An approximation with a high correlation coefficient was produced when the experimental kinetic results of all three metals were tested for the pseudo-first-order model (>0.990). In Table 3, it is observed that the increase in the initial concentration has improved metal ions absorption potential. So, the PFO was slightly higher than the PSO based on statistical results (R^2) (Ahmed *et al.* 2019; Pushpa *et al.* 2019).

3.6. Reusability studies

After completion of adsorption experiments, the spent sorbent is regenerated. This would minimize the utilization of the sorbent and hence minimize the costs of the treatment phase. Consequently, some elutants such as 0.1M HCl, H_2SO_4 and HNO_3, and 0.1M $CaCl_2$ have been used for desorption tests. The elution performance measured was 99.1 98.9 and 98.4% at an S/L ratio of 1 with three consecutive sorption elution cycles for 0.1M HCl while employed for Zn, Ni, Pb-loaded *C.Scalpelliformis* sorbent. Desorption tests provide further proof of pH effects. Metal ions had high adsorption efficiency at pH of 7 for Pb and 6 for Ni and Zn, and a rise in pH reduced adsorption ability. In the desorption studies, the effect of acidic elutants was relatively poor and simple elutants showed a strong efficiency in desorption (Ravindiran *et al.* 2019). Adsorption and desorption are reversible systems, So 0.1M HCl is the most powerful adsorbent elutant for three metal ions.

4. Conclusion

Green seaweed *C.Scalpelliformis* has been identified as an important sorbent for removing metal ions in research. In laboratory experiments, the pH equilibrium was shown to affect the sorption potential of metal ions significantly, and the optimum pH was 7.0 for Pb and 6.0 for Ni and Zn. The optimal temperature and sorbent dosage for removing metal ions were determined to be at room temperature and two g/L. The modelling results showed that relative to the Langmuir, Freundlich and Sips models, the Toth model was considered to be better adapted to experimental results. The level of biosorption was found to be high, and equilibrium was reached in 120 minutes. Implementing metal ion kinetic data on the first-order pseudo model has contributed to an exact fit on the

second-order pseudo model. Finally, we found that HCl is the best elutant, with an overall elutant performance of 99.1%, among the various elutants used. In all the experiments, it is clear that the removal performance of three separate metal ions was in the range of Zn>Ni>Pb. For zinc ions, the maximum removal efficiency was achieved by using *C.Scalpelliformis*. The experimental and modelling data reveal that the *C.Scalpelliformis* sorbent can be considered an ideally suited sorbent for the remediation of metal ions. Desorption experiments also show that the sorbent can be regenerated easily and that no secondary pollutants are created in the environment.

References

Ahmed M.J., Okoye P.U., Hummadi E.H. & Hameed B.H. (2019). High-performance porous biochar from the pyrolysis of natural and renewable Seaweed (*Gelidiella acerosa*) and its application for the adsorption of methylene blue, *Bioresource technology,* **278**, 159–164.

Aravindhan R., Rao J.R. & Nair B.U. (2007). Removal of basic yellow dye from aqueous solution by sorption on green alga *Caulerpa scalpelliformis, Journal of hazardous materials,* **142(1–2)**, 68–76.

Çeçen F. (2018). Removal and behavior of hazardous pollutants in biological treatment systems, *Hazardous Pollutants in Biological Treatment Systems*, 123–182.

Chen Y., Wang B., Xin J., Sun P. & Wu D. (2018). Adsorption behavior and mechanism of Cr(VI) by modified biochar derived from *Enteromorpha prolifera, Ecotoxicology and Environmental Safety,* **164**, 440–447.

Deng S., Wang P., Zhang G. & Dou Y. (2016). Polyacrylonitrile-based fiber modified with thiosemicarbazide by microwave irradiation and its adsorption behavior for Cd(II) and Pb(II), *Journal of Hazardous Materials,* **307**, 64–72.

Deng S., Zhang G., Chen S., Xue Y., Du Z. & Wang P. (2016). Rapid and effective preparation of a HPEI modified biosorbent based on cellulose fiber with a microwave irradiation method for enhanced arsenic removal in water, *Journal of materials chemistry A*, **4**, 15851–15860.

Gao S., Luo T., Zhou Q. & Luo W. (2018). A novel and efficient method on the recovery of nanosized CeO_2 in Ce^{3+} wastewater remediation using modified sawdust as adsorbent, *The Journal of Colloid and Interface Science,* **512**, 629–637.

Gokulan R., Avinash A., Prabhu G.G., & Jegan J. (2019). Remediation of remazol dyes by biochar derived from *Caulerpa scalpelliformis*—An eco-friendly approach, *Journal of environmental chemical engineering,* **7**, 103297.

Gokulan R., Ganesh Prabhu G. & Jegan J. (2019). A novel sorbent *Ulva lactuca*-derived biochar for remediation of Remazol Brilliant Orange 3R in packed column, *Water Environment Research,* **91**, 642–649.

Gokulan R., Prabhu G.G. & Jegan J. (2019). Remediation of complex remazol effluent using biochar derived from green seaweed biomass, *International journal of phytoremediation,* **21(12)**, 1179–1189.

Gupta N.K., Sengupta A., Gupta A., Sonawane J.R. & Sahoo H. (2018). Biosorption-an alternative method for nuclear waste management: A critical review, J*ournal of environmental chemical engineering,* **6(2)**, 2159–2175.

Hua P., Sellaoui L., Franco D., Netto M.S., Luiz Dotto G., Bajahzar A. and Li Z. (2019). Adsorption of acid green and procion red on a magnetic geopolymer based adsorbent: Experiments, characterization and theoretical treatment, *Journal of chemical engineering,* **383**, 123113.

Kanagaraj J., Senthilvelan T., Panda R.C. & Kavitha S. (2015). Eco-friendly waste management strategies for greener environment towards sustainable development in leather industry: a comprehensive review, *Journal of cleaner production*, **89**, 1–17.

Li H., Dong X., da Silva E.B., de Oliveira L.M., Chen Y. & Ma L.Q. (2017). Mechanisms of metal sorption by biochars: Biochar characteristics and modifications, *Chemosphere*, **178**, 466–478.

Liu L., Huang Y., Zhang S., Gong Y., Su Y., Cao J., Hu H. (2019). Adsorption characteristics and mechanism of Pb(II) by agricultural waste-derived biochars produced from a pilot-scale pyrolysis system, *Journal of waste management*, **100**, 287–295.

Yusuf M., Ed., (2018). Handbook of Textile Effluent Remediation, *Pan Stanford Publishing Pvt. Ltd., Singapore.*

Maiti D., Ansari I., Rather M.A. & Deepa A. (2019). Comprehensive review on wastewater discharged from the coal-related industries – characteristics and treatment strategies, *Water Science and Technology*, **79**, 2023–2035.

Mazur L.P., Cechinel M.A.P., de Souza S.M.A.G.U., Boaventura R.A.R. & Vilar V.J.P. (2018). Brown marine macroalgae as natural cation exchangers for toxic metal removal from industrial wastewaters: A review, *Journal of Environmental Management,* **223,** 215–253.

Praveen R.S. & Vijayaraghavan K. (2014). Optimization of Cu(II), Ni(II), Cd(II) and Pb(II) biosorption by red marine alga *Kappaphycus alvarezii*, *desalination and water treatment,* **55(7)**, 1816–1824.

Prodromou M. & Pashalidis I. (2015). Europium adsorption by non-treated and chemically modified *opuntia ficus indicacactus* fibres in aqueous solutions, *Desalination and Water Treatment,* **57**, 5079–5088.

Pushpal T.B., Josephraj J., Saravanan P. & Ravindran G. (2019). Biodecolorization of Basic Blue 41 using EM based Composts: Isotherm and Kinetics, *ChemistrySelect,* **4(34)**, 10006–10012.

Rahman M.L., Biswas T.K., Sarkar S.M., Yusoff M.M., Sarjadi M.S., Arshad S.E. & Musta B. (2017). Adsorption of rare earth metals from water using a kenaf cellulose-based poly (hydroxamic acid) ligand, *Journal of molecular liquids,* **243**, 616–623.

Rangabhashiyam S., Giri Nandagopal M.S., Nakkeeran E., Keerthi R. & Selvaraju N. (2016). Use of Box–Behnken design of experiments for the adsorption of chromium using immobilized macroalgae, *Desalination and Water Treatment,* **57**, 26101–26113.

Rangabhashiyam S., Suganya E., Selvaraju N. & Varghese L.A. (2014). Significance of exploiting non-living biomaterials for the biosorption of wastewater pollutants, *World Journal of microbiology and biotechnology,* **30**, 1669–1689.

Ravindiran G., Ganapathy G.P., Josephraj J. & Alagumalai A. (2019). A Critical Insight into Biomass Derived Biosorbent for Bioremediation of Dyes, *ChemistrySelect*, **4(33)**, 9762–9775.

Ravindiran G., Jeyaraju R.M., Josephraj J. & Alagumalai A. (2019). Comparative Desorption Studies on Remediation of Remazol

Dyes Using Biochar (Sorbent) Derived from Green Marine Seaweeds, *ChemistrySelect*, **4**(**25)**, 7437–7445.

Sagar S. & Rastogi A. (2019). Evaluation of Equilibrium Isotherms and Kinetic Parameters for the Adsorption of Methyl Orange Dye onto Blue Green Algal Biomass, *Asian journal of chemistry,* **31(7)**, 1501–1508.

Senthilkumar R., Prasad D.M.R., Govindarajan L., Saravanakumar K. & Prasad B.S.N. (2017). Green alga-mediated treatment process for removal of zinc from synthetic solution and industrial effluent, *Environmental technology,* **40**, 1262–1270.

Torab-Mostaedi M., Asadollahzadeh M., Hemmati A. & Khosravi, A. (2013). Biosorption of lanthanum and cerium from aqueous solutions by grapefruit peel: equilibrium, kinetic and thermodynamic studies, *Research on Chemical Intermediates,* **41**, 559–573.

Vijayaraghavan K. & Ashokkumar T. (2017). Plant-mediated biosynthesis of metallic nanoparticles: A review of literature, factors affecting synthesis, characterization techniques and applications, *J. Environ. Chem. Eng,* **5(5)**, 4866–4883.

Vijayaraghavan K., Rangabhashiyam S., Ashokkumar T. & Arockiaraj J. (2017). Assessment of samarium biosorption from aqueous solution by brown macroalga *Turbinaria conoides*, *Journal of the Taiwan Institute of Chemical Engineers*, **74**, 113–120.

Xu W. & Duran M. (2018). Removal of hazardous pollutants in full-scale wastewater treatment plants, *Hazardous Pollutants in Biological Treatment Systems*, 239–263.